

## Seismic-Moment Tensor of Earthquakes in Azerbaijan for 2012–2015

G.J. Yetirmishli, S.E. Kazimova, I.E. Kazimov

Azerbaijan National Academy of Sciences, Republican Center for Seismological Survey  
123, ul. Gusein Javida, Baku, Az 1001, Azerbaijan

Received 17 August 2017; accepted 11 June 2018

**Abstract**—Seismic-moment tensor solutions for earthquakes in Azerbaijan for 2012–2015 have been calculated with a new method by full waveform inversion of broadband data from modern digital seismic stations and processed statistically. The results are used to model main faulting elements in the region, to correlate the seismicity and fault patterns, and to compile a map of fault plane orientations for large events. The principal compression stress (P) directions are NW to SE in the Zaqatala area and N–S in the Sheki area but then gradually change clockwise toward NE–SW in the Caspian Sea. The directions of principal extension are mainly NE–SW and N–S within the zone where the Kura basin is subsiding beneath the Great Caucasus.

**Keywords:** seismology, earthquakes, compression and extension stress axes, Azerbaijan

### INTRODUCTION

The focal mechanism is a key characteristic of an earthquake. In the modern seismology, the earthquake source is interpreted as an instantaneous slip of rocks accompanied by radiation of seismic energy and propagation of waves along the surface of weakness. Earthquake mechanisms provide the essential part of information on crustal stress (Melnikova and Radziminovich, 1999): they show the spatial orientations of principal stresses (compression (P) and extension (T) axes), possible slip planes, and slip vectors at the source. The recovered stress and strain patterns, along with geological and structural data, allow modeling crustal deformation processes (Sycheva, 2004).

The first idea of stress distribution in the Great Caucasus region came from publications by Gotsadze and Shirokova in 1952 through 1959. The studies of the present stress and strain fields based on earthquake focal mechanisms in the territory of Azerbaijan began in the 1960s due to efforts of Russian scientists (Vvedenskaya, Balakina, Misharina, Solonenko, and others) and were taken up by Azerbaijan seismologists (Agalarova in 1963 through 1993 and Agaeva in 1978 through 2007).

Currently the dense regional network of thirty five digital seismic stations can record all  $M > 0.1$  events within Azerbaijan and furnish new data for calculating earthquake focal mechanisms with implications for the ongoing lithospheric deformation.

The studies of stress and strain are of special practical value as a basis for seismic risk assessment in zones of civil and industrial facilities, including oil and gas fields.

This paper is a synthesis of seismic-moment tensor solutions obtained by waveform inversion of broadband data from digital seismic stations using advanced algorithms, for large earthquakes that occurred in Azerbaijan for the 2012–2015 period.

### GEOLOGICAL BACKGROUND

The territory of Azerbaijan is located in the eastern Caucasus segment of the Alpine orogenic system. In the east it borders the vast N–S trending basin of the Caspian Sea; the northern flank of the region corresponds to the eastern part of the southern Great Caucasus uplift and the adjacent zone of subsidence in the southeast. Central Azerbaijan is occupied by the Kura intermontane basin which accommodates thick Neogene–Anthropogene molasse. The molasse deposits are deformed into steep folds which are partly thrust southward south of the Alazani–Agrichay basin and form low brachianticlinal uplifts within the Kura–Araks basin (Mamedov et al., 2005).

On a global scale, the territory comprises three large blocks of the central Crimea–Caucasus–Kopetdagh Alpine orogenic system which make up the framework of Azerbaijan’s major structural units (Aslanov, 2009): the Dasht-e Lut block in eastern Iran, the Central Caspian–Turan plate on the eastern side of the Central Caspian Sea, and the Main Zagros fold-thrust belt in the southwestern Iran.

An earthquake is a mechanic failure process of rupture and slip of stressed rocks on a fault plane in the crust. Earth-

✉ Corresponding author.

E-mail address: sabina.k@mail.ru (G.J. Yetirmishli)

quake focal mechanisms are commonly analyzed with reference to maps of faults, and the choice of a reference map is of special importance. In this study we use the tectonic map of Azerbaijan compiled on the basis of published data (Shikhaliyev, 1996; Kengerli, 2007; Rzaev et al., 2013).

## METHODS

The reported full waveform inversion was performed using the Time-Domain Moment Tensor INverseCode (TDMT INVC) of Dreger (2002). Most of data have been collected by the Azerbaijan Republican Center for Seismological Survey. Seismograms are downloaded in the SEED format and converted to SAC data files. Broadband records are selected with limitations on distance (70 to 350 km), du-

ration ( $P$ - to  $S$ -wave interval), and quality (high signal/noise ratio, no clipping). The preparation of seismograms for inversion includes: picking  $P$  arrivals; restoring the original ground motion by time-domain deconvolution; estimating epicentral distance and azimuth from epicenter to station and back; calculating radial and transverse components; and 4th-order Butterworth bandpass filtering (Fig. 1).

The work begins with reading the files of parameters, station coordinates, and output location followed by several operations: (1) correcting waveforms for instrument response and conversion of N–S, E–W, and vertical coordinates to radial, tangential, and vertical coordinates; (2) 4th-order Butterworth bandpass filtering; (3) calculating Green's functions used for synthetic waveform inversion for the whole set of origin depths and offsets (obtained with the real-time location program); (4) applying Fourier transform

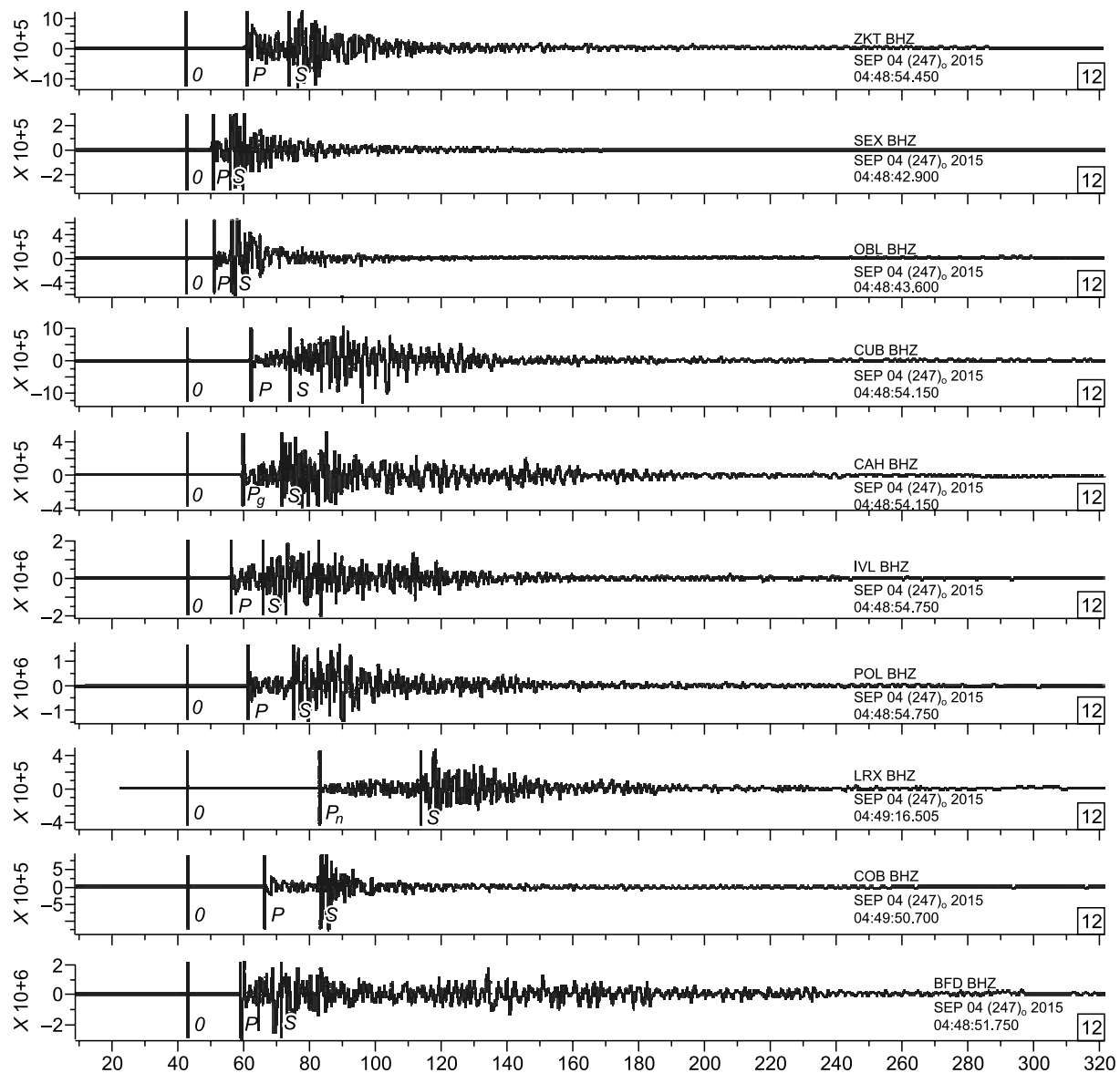


Fig. 1. SAC broadband record of the  $M = 5.9$  earthquake of 04.09.2015.

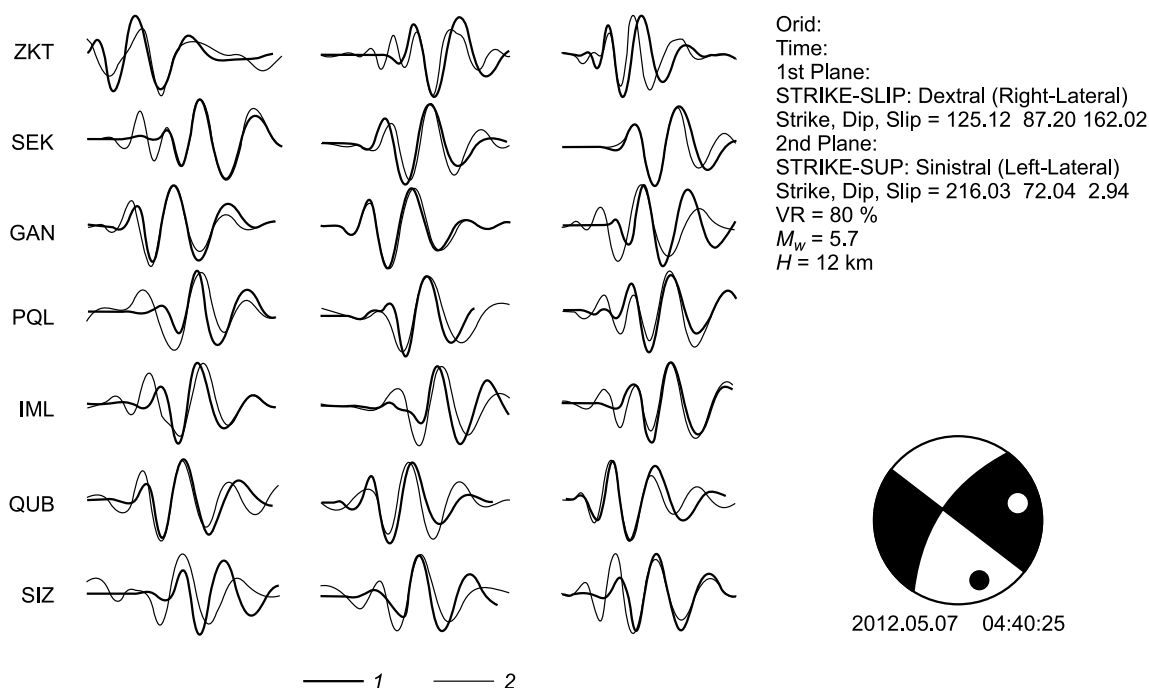


Fig. 2. Real (1) and synthetic (2) waveforms and fault plane solution for the  $M = 5.6$  earthquake of 07.05.2012.

for frequency-to-time domain conversion of Green function components, in order to create the respective files for the given set of distances; (5) 4th-order Butterworth bandpass filtering of the Green functions; (6) TDMT inversion and calculation of seismic-moment tensors and  $M_w$  magnitudes (Fig. 2) of events (Kushnir et al., 2010).

Although an earthquake source is actually an elongate object, it is commonly characterized as a point in the first approximation. This approach is valid at wavelengths largely exceeding the geometrical size of the source and at time periods much longer than the failure process. In practice, these assumptions are fulfilled only approximately.

The reference 1D velocity model was based on traveltimes of compressional and shear wave components  $P$ ,  $Pg$ ,  $Pn$ ,  $S$ ,  $Sg$  and  $Sn$  from  $M_l \geq 2.5$  earthquakes recorded by the network of telemetric stations for the period from 2005 to 2012. The data were processed in VELEST, the software for traveltimes inversion to 1D velocity models (Yetirmishli and Kazimova, 2012). The study covered the Greater Caucasus, Lower Kura basin, Shamakhi–Ismayilly, and the Caspian Sea areas (Table 1).

Thus we calculated and analyzed the mechanisms of  $M \geq 4.0$  earthquakes that occurred in the four areas of the region between 2012 and 2015. The results were used to reveal features of seismotectonic deformation in the Zaqatala, Sheki, Qabala, Oghuz, Hacıqabul, Ismayilly, and Caspian Sea seismogenic zones of Azerbaijan (Fig. 3; Table 2). fault plane solutions are presented as beachball stereograms (Fig. 4) on the simplified fault map of the region (Shikhali-beili et al., 1996).

## LARGE EARTHQUAKES IN AZERBAIJAN, 2012–2015

Earthquake of 7 May 2012,  $M_l = 5.6$ , Zaqatala area: nearly horizontal ( $PL_p = 10^\circ$ ) compression and extension ( $PL_T = 14^\circ$ ); strike slip on both high-angle planes dipping at  $DP_1 = 87^\circ$  and  $DP_2 = 72^\circ$ ; right-lateral strike slip on the first nodal plane  $NP1$  oriented in the SE direction ( $STK_1 = 125^\circ$ ) and left-lateral strike slip on the SW second plane  $NP2$  ( $STK_2 = 216^\circ$ ). The plane  $NP1$  follows the Gazakh–Signagi and Ganjachay–Alazani right-lateral strike slip faults running across the Caucasus Range, i.e., the  $NP2$  plane was responsible for the earthquake. On the same day, another event of a similar magnitude ( $M_l = 5.7$ ) occurred under nearly horizontal extension ( $PL_T = 1^\circ$ ) as normal slip with a right-lateral strike-slip component on the  $NP1$  plane and with a left-lateral strike-slip component on  $NP2$ . One more  $M_l = 5.0$  shock recorded on 18 May 2012 in the area had the same mechanism: a normal slip with a strike-slip component (Fig. 5).

Two more events on 7 October of 2012: a  $M_l = 5.3$  earthquake in the Ismayilly area and a  $M_l = 5.7$  event in the Balakan area, both under nearly horizontal extension ( $PL_T = 0^\circ$ ). The mechanism likewise corresponded to a normal slip with a strike-slip component (Fig. 6). The motion in the Ismayilly event was associated with the activity of the North Ajinohur fault.

According to solutions of the USGS, CPP, GFZ, and HARV international seismological centers, the two Zaqatala shocks (GMT 4:40,  $M_w = 5.6$  and GMT 14:15,  $M_w = 5.7$ )

**Table 1.** Velocity model taken for reference in inversion for fault plane solutions

Depths, km	Density, g/cm <sup>3</sup>	Velocity, km/s		Depths, km	Density, g/cm <sup>3</sup>	Velocity, km/s	
		<i>P</i> waves	<i>S</i> waves			<i>P</i> waves	<i>S</i> waves
Greater Caucasus				Lower Kura basin			
3	2.3	3.88	2.25	3	2.3	3.99	2.09
5	2.4	4.21	2.57	5	2.4	4.2	2.18
7	2.5	4.38	2.57	8	2.5	4.2	2.41
10	2.7	5.9	3.26	10	2.7	5.32	3.56
15	2.9	6.4	3.55	15	2.9	6.2	3.57
23	2.9	6.68	3.82	25	2.9	7.33	4.25
34	3.0	7.09	3.97	35	3.0	7.76	4.25
44	3.0	7.35	3.97	40	3.1	7.76	4.46
50	3.0	7.52	4.64	50	3.1	7.88	4.48
60	3.3	8.52	4.79	70	3.1	7.92	4.48
Shamakhi-Ismayilly area				Caspian Sea			
3	2.3	3.62	2.33	3	2.2	3.34	2.06
5	2.4	4.21	2.43	5	2.4	3.34	2.06
8	2.5	4.49	2.64	8	2.5	3.56	2.25
10	2.7	5.04	3.19	10	2.7	5.53	3.50
15	2.9	6.02	3.53	15	2.9	5.91	3.50
25	3.0	7.97	4.11	25	3.0	7.34	4.23
35	3.0	7.97	4.12	35	3.0	7.35	4.23
40	3.0	7.97	4.41	40	3.1	7.85	4.43
50	3.3	8.13	4.48	50	3.3	8.31	4.66
70	3.3	8.16	4.59	70	3.3	8.39	4.73

had reverse and normal slip mechanisms, respectively, and originated from the same source (the same origin depth of 10 km and the epicenter location), while the Balakan event (GMT 14:15,  $M_w = 5.7$ ) occurred as a reverse slip (Figs. 7, 8). This is an unusual case in terms of tectonics and geody-

namics (Rzaev and Metaksas, 2011), more so that detailed calculations at the Republican Seismological Center lead to different source parameters.

According to Rzaev and Metaksas (2011), the thrusts observed on the surface in the Shamkir–Zaqatala zone with a

**Table 2.** Earthquake mechanism parameters,  $M_l \geq 4.0$  events, 2012–2015

No.	Data, year, month, day	$t_0$ , hr:min:s	$H$ , km	$M_l$	$M_w$	Location		Nodal planes					
						N	E	NP1			NP2		
								<i>STK</i>	<i>DP</i>	<i>SLIP</i>	<i>STK</i>	<i>DP</i>	<i>SLIP</i>
1	2012.05.07	04:40:25	9	5.6	5.9	41.50	46.58	125	87	162	216	72	2
2	2012.05.07	14:15:13	12	5.7	5.3	41.56	46.63	130	48	-117	349	48	-62
3	2012.05.18	14:46:33	13	5.0	5.1	41.53	46.62	354	47	-68	144	47	-111
4	2012.10.07	11:42:50	41	5.3	5.1	40.70	48.35	128	45	-81	295	45	-98
5	2012.10.14	10:13:36	8	5.7	5.6	41.66	46.27	116	58	-141	2	58	-39
6	2013.04.06	09:19:36	26	4.0	3.8	40.98	46.67	286	81	108	40	20	24
7	2013.04.18	20:38:51	25	4.5	4.6	41.10	47.28	54	85	6	323	83	175
8	2013.04.30	09:29:34	10	4.2	4.3	40.44	48.02	254	72	-38	357	53	-158
9	2014.02.10	12:06:19	46	5.7	5.5	40.23	48.62	125	59	-57	253	44	-132
10	2014.06.07	06:05:20	61	5.6	5.4	40.13	51.66	119	66	-59	243	38	-139
11	2014.06.29	17:26:07	9	5.2	5.0	41.54	46.54	241	79	-15	334	75	-169
12	2014.09.29	01:38:07	11	5.5	5.1	41.13	47.94	265	64	-43	17	53	-146
13	2014.10.03	09:45:06	8	4.0	4.0	41.24	45.61	354	58	120	127	43	52
14	2014.10.04	04:59:32	6	5.0	4.9	41.11	47.94	268	82	-25	1	65	-171
15	2015.09.04	04:49:36	16	5.9	5.5	40.97	47.43	153	90	-180	63	90	0

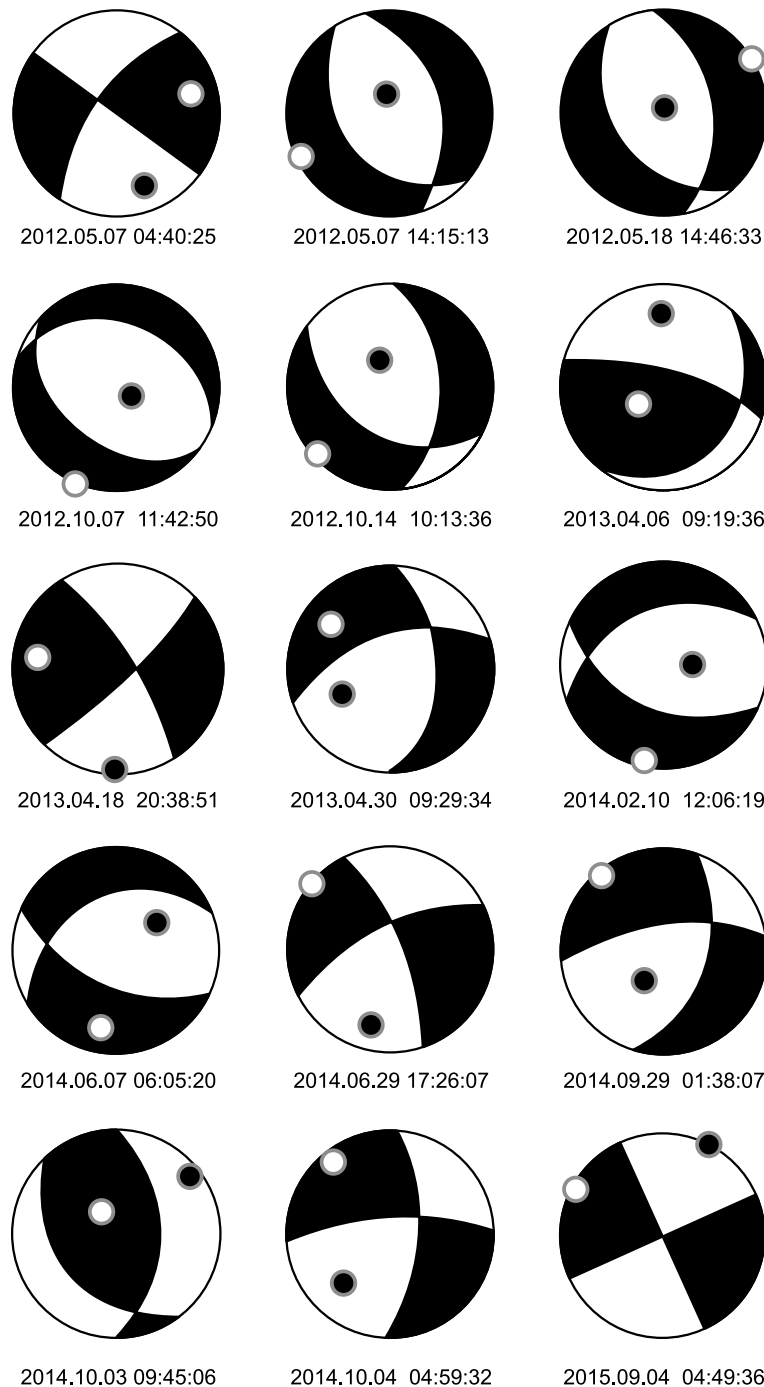


**Fig. 3.** Focal mechanisms of  $M \geq 4.0$  earthquakes in Azerbaijan that occurred in 2012–2015.

shallow pre-Alpine basement within the Greater Caucasus uplift, are quite shallow and exert no effect on the local seismicity which is rather controlled by steep normal faults along southern and northern sides of the uplifted basement blocks rich in magnetic rocks, as well as with cross-Caucasian strike-slip faults. The reverse and thrust faults are seismogenic, as well as normal faults, east of the Ganjachay–Alazani fault, where the pre-Alpine basement surface is deeper (8 km) and does not preclude depthward propagation

of reverse and thrust faulting under general compression of the Greater Caucasus (Fig. 9).

Thus, we infer that the Zaqatala events originated under the effect of faults running along and across the general strike of the Caucasus Range (Caucasian and cross-Caucasian, respectively), especially on the Gazakh–Signagi and Ganjachay–Alazani right-lateral strike-slip faults in the latter case.

The discussed earthquakes had normal slip mechanisms with a left-lateral strike slip component. The latter solution

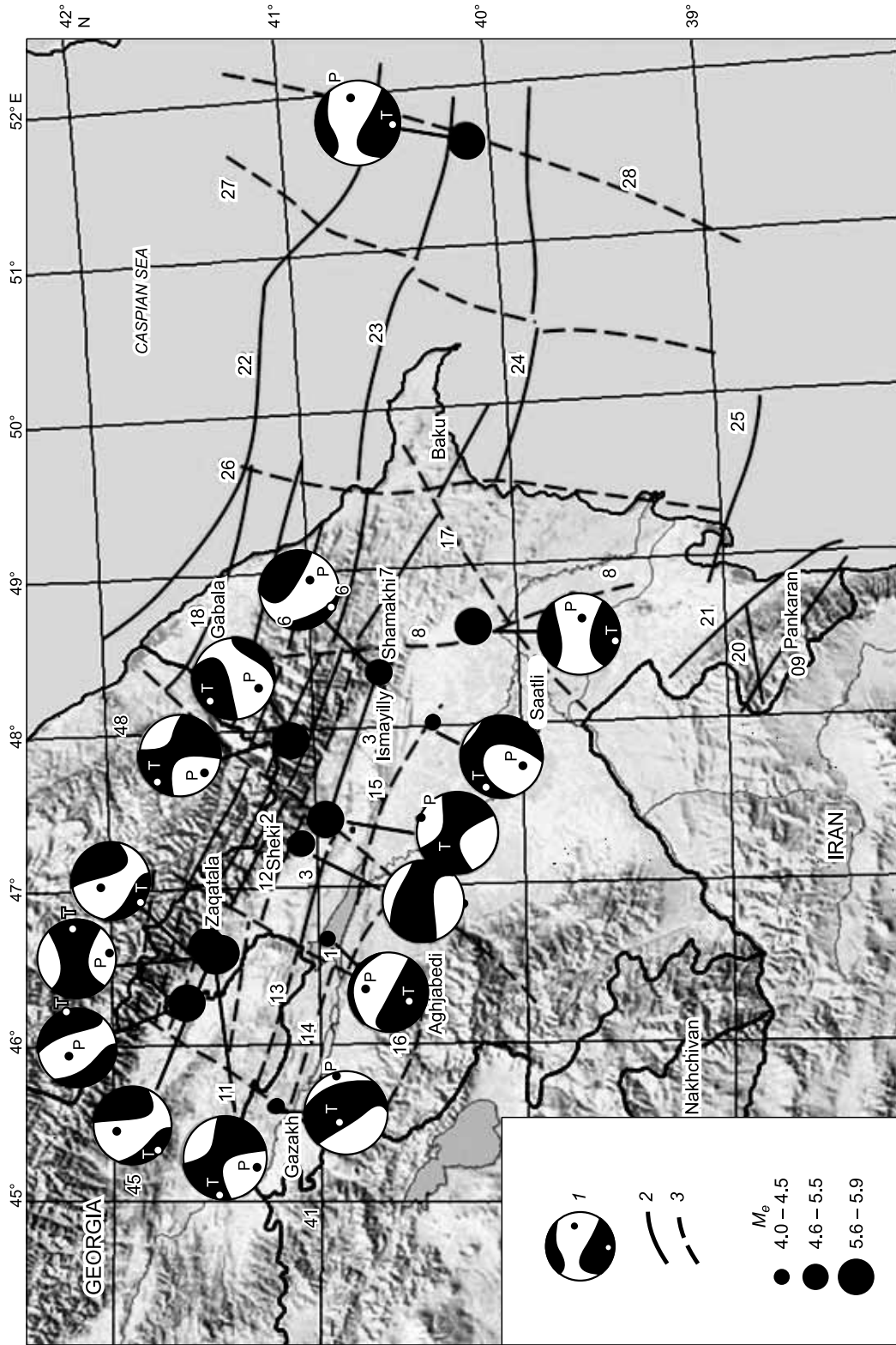


**Fig. 4.** Faults and focal mechanisms of  $M_f \geq 4.0$  earthquakes of 2012–2015. 1, earthquake mechanism stereoplots; 2, reverse faults; 3, normal and strike-slip faults. Arabic numerals stand for fault names: 1, Dashgil–Mudresu; 2, Vandam; 3, Goychay; 4, Siazan; 5, Zangi–Kozluchay; 6, Germian; 7, Ajichay–Aliat; 8, West Caspian; 9, Arpa–Samur; 10, Ganjachay–Alazani; 11, Gazakh–Signagi; 12, North–Ajinohur; 13, Iori; 14, Kura; 15, Mingachevir–Saatli; 16, Bashlybel; 17, Palmira–Absheron; 18, Akhty–Nyugdi–Kiliazi; 19, Talysh; 20, Yardymli; 21, Fore–Talysh; 22, Central Caspian; 23, Absheron–Balkan; 24, Sanqachal–Ogurji; 25, Mil–Chikishlar; 26, Yashmi flexure; 26a, Kizilagbek; 27, Shakhly–Azizbek; 28, Garabogaz–Sefidrud.

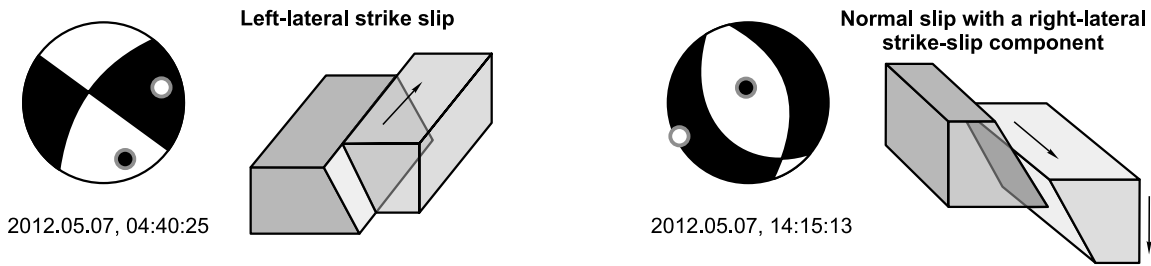


Fig. 5. Mechanisms of Zaqatala earthquakes of 2012 and slip models: NP1 (2012.05.07, 14:15:13) and NP2 (2012.05.07, 04:40:25).

appears preferable, especially for the Zaqatala event, as a W–E (Caucasian) reverse slip, as well as pure normal slip without any horizontal component for the second shock, are inconsistent with the geodynamic model of the area.

The solutions of the USGS, CPP, GFZ, and HARV international seismological centers suggest a reverse slip mechanism for the Ismayilly earthquake (Fig. 10), as in the case of the previous events.

The Shamakhi–Ismayilly seismic area is located in the southeastern Greater Caucasus and has a complex piano-key stepped structure. The fault steps in the pre-Alpine basement are presumably cut by steep Caucasian and cross-Caucasian faults that delineate subsided and uplifted blocks (Akhmedbeili et al., 2010) and grade into low-angle reverse and thrust faults in Mesozoic and Cenozoic sediments.

In the map of faults (Fig. 11) compiled for the Shamakhi–Ismayilly source area with reference to published data (Kengerli, 2007; Kerimov and Shihalibeili, 1992), the earthquake falls within the West Caspian and North Ajinohur oblique faults. This location provides additional evidence

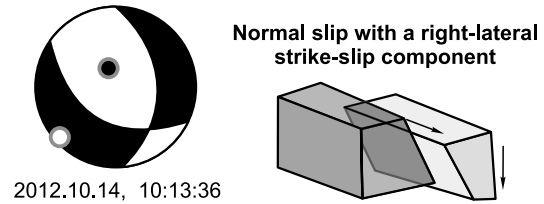


Fig. 6. Mechanism of Balakan earthquake of 2012 and slip model.

for high local seismicity and large depth of the West Caspi-an normal fault with a right-lateral strike slip component.

The magnitude of earthquakes in 2013 never exceeded  $M = 5$ , but there were three notable events in the Mingachevir (2013.04.06), Sheki (2013.04.18), and Kurdamir (2013.04.30) areas. The motion in the Mingachevir event had reverse slip geometry with a right-lateral strike-slip component along the NP1 plane and normal slip with a left-lateral strike slip component along NP2. The nodal planes dip from  $81^\circ$  to  $20^\circ$  and are oriented in the northwestern

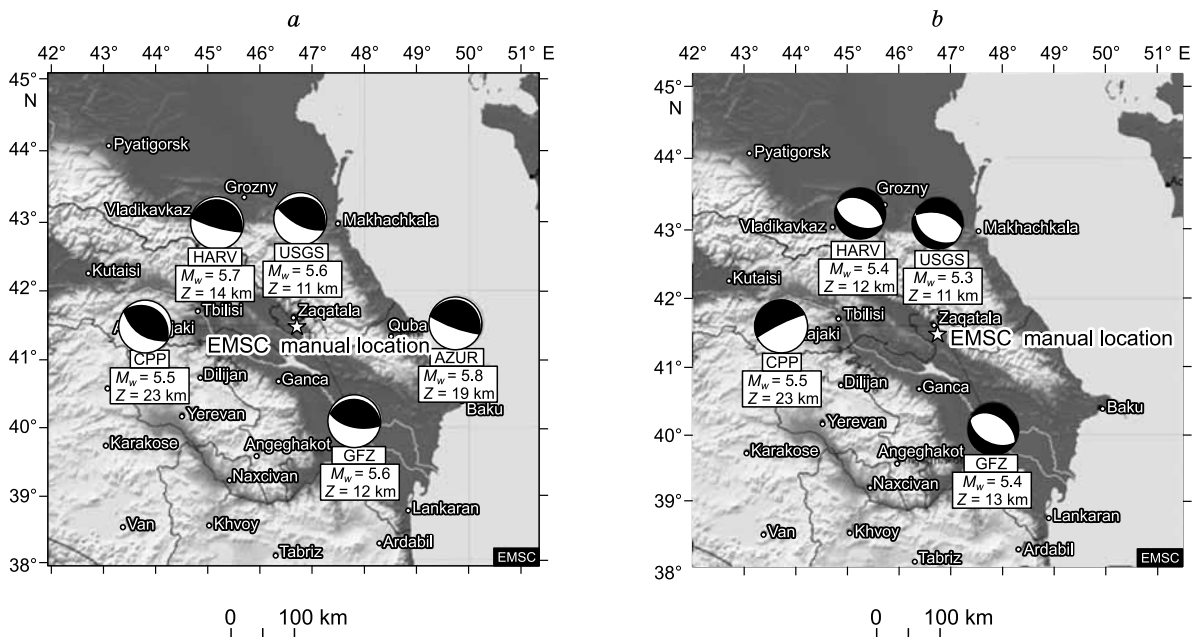
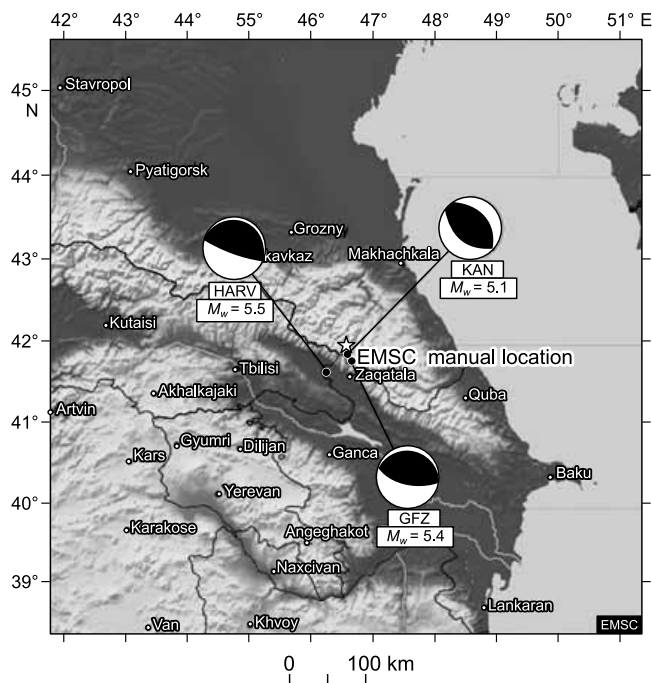


Fig. 7. Mechanisms of Zaqatala earthquakes of 2012 according to data of international seismological centers:  $M_w = 5.6$  event at 4:40 GMT (a) and  $M_w = 5.7$  event at 14:15 GMT.



**Fig. 8.** Mechanism of Balakan earthquake of 2012 according to data of international seismological centers:  $M_w = 5.4$  event at 10:13 GMT.

( $NP_1$ ) and northeastern ( $NP_2$ ) directions; only  $NP_1$  agrees with the strike of the Goychay fault. The geometry of motion was strike slip with a reverse component on both planes (Vandam fault) in the Sheki earthquake and normal slip with a strike slip component along the Mingachevir–Saatli fault in the Kurdamir event.

Earthquake of 10 February 2014, Hacıqabul area: nearly vertical ( $PL_p = 61^\circ$ ) ENE compression ( $AZM = 87^\circ$ ) and nearly horizontal ( $PL_p = 8^\circ$ ) SSW extension ( $AZM = 192^\circ$ );

normal slip with a strike-slip component on both planes ( $DP_1 = 59^\circ$  and  $DP_2 = 44^\circ$ ); the nodal planes have NE ( $NP_1$ ) and SW ( $NP_2$ ) orientations at  $STK_1 = 125^\circ$  and  $STK_2 = 253^\circ$ , respectively. The  $NP_2$  plane (Fig. 4) is parallel to two existing faults (Kura and Ismayilly–Qabala) and hence must be responsible for the shock.

Caspian earthquake of 7 June 2014: nearly horizontal extension ( $PL_T = 15^\circ$ );  $NP_1$  and  $NP_2$  of SE ( $STK_1 = 119^\circ$ ) and SW ( $STK_2 = 243^\circ$ ) orientations, respectively; normal slip with a strike-slip component on both planes ( $DP_1 = 66^\circ$ ,  $DP_2 = 38^\circ$ ), along the Absheron–Balkan fault.

Earthquake of 29 June 2014 in the Zaqatala–Balakan area,  $M_l = 5.3$ : nearly horizontal compression ( $PL_p = 18^\circ$ ) and extension ( $PL_T = 3.0^\circ$ ) directed to the southwest ( $AZM = 197^\circ$ ) and northwest ( $AZM = 288^\circ$ ); strike slip on both planes dipping steeply at  $DP_1 = 79^\circ$  and  $DP_2 = 75^\circ$ ; nearly W–E and N–S orientations of  $NP_1$  ( $STK_1 = 241^\circ$ ) and  $NP_2$  ( $STK_2 = 334^\circ$ ), respectively.  $NP_1$  following the cross-Caucasian right-lateral strike slip faults of Gazakh–Signagi and Ganjachay–Alazani (Fig. 6) was seismogenic.

Two  $M_l = 5.5$  and  $M_l = 5.0$  earthquakes of 29 September and 4 October 2014 occurred northeast of Qabala. Event 1: high-angle ( $PL_p = 48^\circ$ ) SW ( $AZM = 265^\circ$ ) compression; normal slip with a strike-slip component on both planes ( $DP_1 = 64^\circ$ ,  $DP_2 = 53^\circ$ );  $NP_1$  and  $NP_2$  oriented, respectively, in the W–E ( $STK_1 = 265^\circ$ ) and N–S ( $STK_2 = 17^\circ$ ) directions;  $NP_2$  parallel to the Ismayilly–Qabala fault (Fig. 6).

Event 2: low-angle ( $PL_p = 23^\circ$ ) compression; strike slip with a normal slip component; W–E ( $STK_1 = 268^\circ$ ) and N–S ( $STK_2 = 1^\circ$ ) orientations of the  $NP_1$  and  $NP_2$  planes, respectively;  $NP_1$  parallel to the cross-Caucasian Arpa–Samur fault (Fig. 6), which was most likely the causative structure.

The  $M_l = 4.03$  event of 3 October 2014 in the Gazakh area: mainly compression; reverse slip with a right-lateral

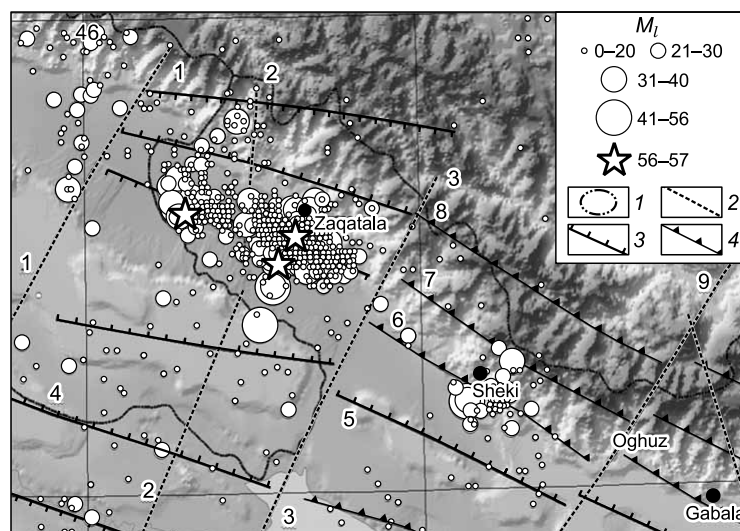


**Fig. 9.** Earthquakes in the Zaqatala–Balakan area in 2012 and fault pattern of the southern slope of the Greater Caucasus. 1, aftershocks; 2, strike slip faults; 3, normal faults; 4, reverse faults. Arabic numerals stand for fault names: 1, Gazakh–Signagi; 2, Sharur–Zaqatala; 3, Ganjachay–Alazani; 4, Iori; 5, North Ajinohur; 6, Vandam; 7, Dashgil–Mudresu; 8, Zangi–Kozluchay; 9, Arpa–Samusy.

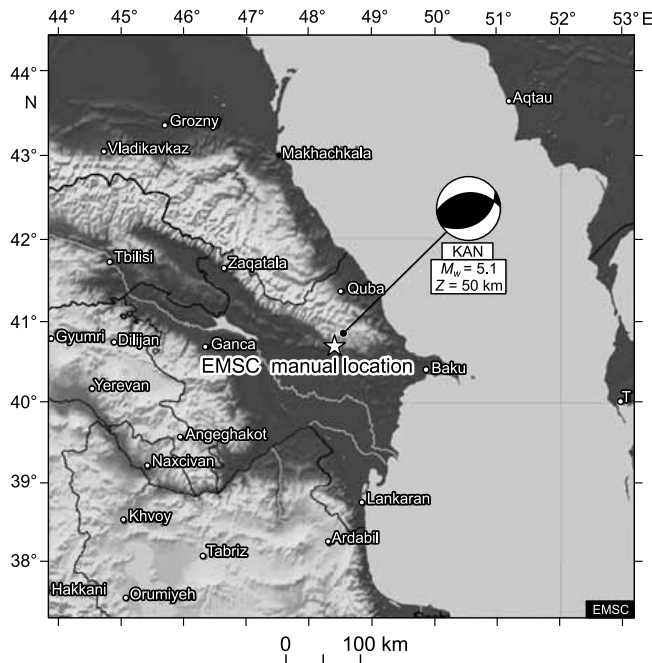


**Fig. 10.** Mechanism of Ismayilly earthquake of 2012 according to data of international seismological centers:  $M_w = 5.1$  event at 11:42 GMT.

strike-slip component on the north-striking plane  $NP1$  and reverse slip with a left-lateral strike-slip component on the NE plane  $NP2$ ; both nodal planes agree with the Zangi–Kozluchay reverse fault with a thrust component.

The earthquake of 4 September 2015 in the Oghuz area, one of largest events over the recent decade, was recorded by 18 international agencies at almost 400 seismic stations worldwide, within distances from 300 to 13,407 km. Ac-

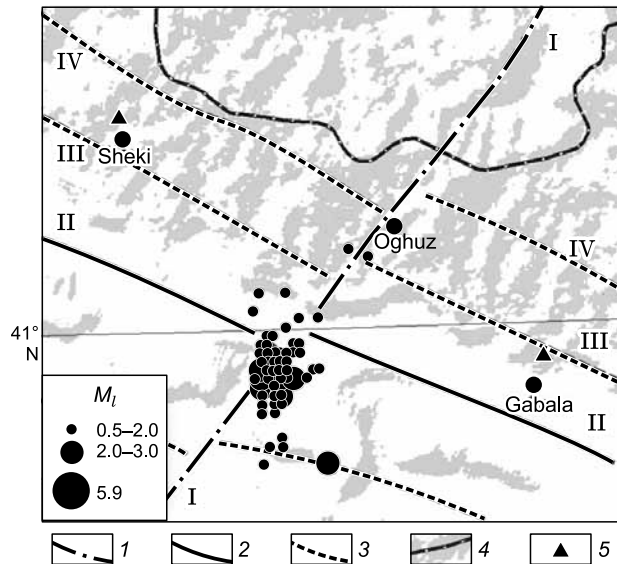


**Fig. 12.** Aftershocks of the  $M_l = 5.9$  Oghuz earthquake of 4 September 2015. Roman numerals stand for fault names: I, Arpa–Samur; II, North Ajinohur; III, Vandam; IV, Dashgil–Mudresu. 1, strike-slip faults; 2, normal faults; 3, reverse faults; 4, national frontier; 5, seismic stations.

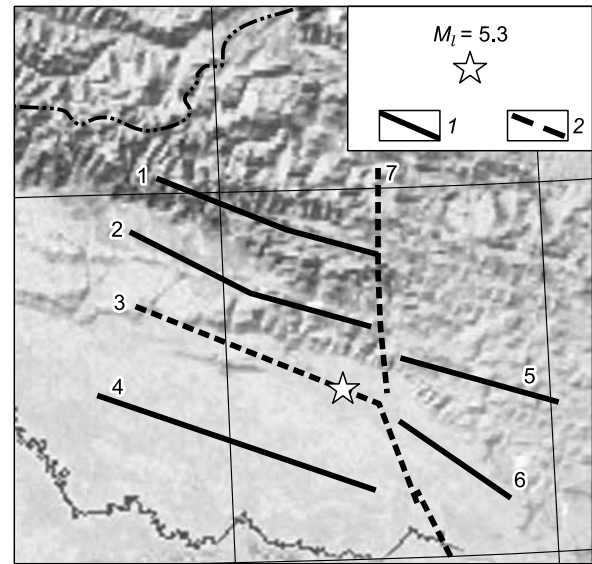


**Fig. 11.** Fault pattern of the Shamakhi–Ismayilly source area (Metaksas et al., 2011). 1, reverse faults; 2, normal and strike slip faults. Arabic numerals stand for fault names: 1, Dashgil–Mudresu; 2, Vandam; 3, Goychay; 4, Zangi–Kozluchayi; 5, Germian; 6, Ajichay–Aliat; 7, West Caspian.

ording to macroseismic evidence, the event was most strongly felt in the Oghuz and Sheki areas: shaking intensity 7 on the MSK-64 scale. The earthquake was followed by more than eighty  $M = 0.5$  to  $M = 4$  aftershocks, 33 shocks within 24 hours after the main shock; the largest ( $M_l = 4.0$ ) aftershock occurred on 13 October at 00:13 local time). The earthquake originated (Fig. 12) at the intersection of the Caucasian Dashgil–Mudresu and cross-Caucasian Arpa–Samur faults (Shikhalibeili, 1996; Kengerli, 2007). The large and old Arpa–Samur fault has been a major tectonic agent in the region since the Paleozoic, which has acted as a conduit for magma and ore-bearing fluids and was the caus-

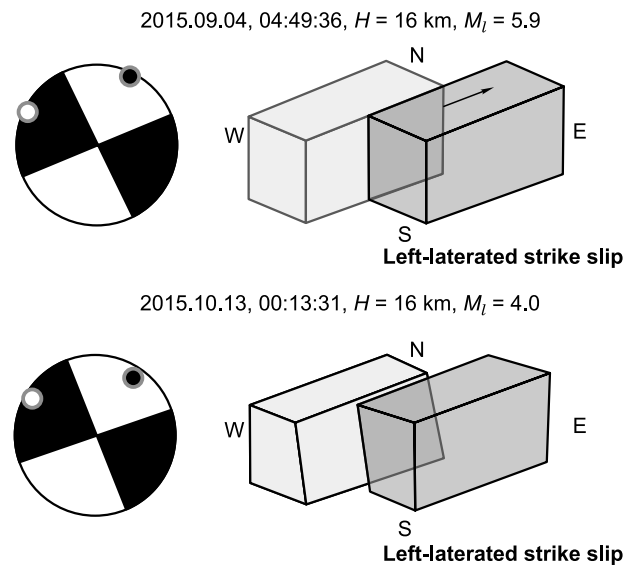


**Fig. 13.** Earthquake mechanisms and slip models,  $NP2$ .

**Table 3.** Earthquake mechanism parameters,  $M_l = 5.9$ –4.0 Oghuz events, 2016

Data, year, month, day	$t_0$ , hr:min:s	$H$ , km	Magnitude			Principal stresses						Nodal planes					
			$M_l$	$M_b$	$M_w$	T		N		P		NP1			NP2		
						$PL$	$AZM$	$PL$	$AZM$	$PL$	$AZM$	$STK$	$DP$	$SLIP$	$STK$	$DP$	$SLIP$
2015.09.04	04:49:36	16	5.9	5.4	5.5	0	288	90	171	0	18	153	90	–180	63	90	0
2015.10.13	00:13:31	16	4.0	–	–	2	287	82	180	7	18	153	86	–172	63	83	–4

ative fault for many earthquakes. The Arpa–Samur trans-Caucasian seismogenic and metalliferous fault zone comprises the deep Murovdagh–Zod, Tartar, and Hacı faults (Shikhalibeili, 1996).

Fault plane solutions were plotted and analyzed for two events in the Oghuz area: the  $M_l = 5.9$  main shock and its largest  $M_l = 4.0$  aftershock under commensurate compression and extension stresses. The NP1 and NP2 planes have SE and NE orientations at  $153^\circ$  and  $63^\circ$ , respectively (Table 3). Compression at the source was directed to the northeast (azimuth  $18^\circ$ ) and acted nearly horizontally ( $0^\circ$ – $7^\circ$ ) while extension was in the WSW direction (azimuth  $287^\circ$ – $288^\circ$ ) at  $0^\circ$ – $2^\circ$  to the horizon. The Oghuz earthquakes occurred as left-lateral strike slip on the Arpa–Samur fault (see Fig. 13 for their mechanisms and a model of slip on the NP2 plane).

The aftershocks migrated in the NE direction (Fig. 14) along a cross-Caucasian fault and reached a depth of 35 km. The mechanisms of two other aftershocks (events of 2015.09.04 and 2015.09.29, both  $M_l = 3.3$ ) show normal slip associated with the North-Ajinohur normal fault.

Comparative analysis of fault plane solutions by different world seismological centers for the two earthquakes recorded by 18 agencies shows that the seismic-moment tensor obtained by the Azerbaijan Seismological Survey Center fits the best the solutions of USGS and GFZ (Fig. 15).

## DISCUSSION

All  $M \geq 4.0$  earthquakes that occurred for 2012 to 2015 in Azerbaijan were grouped according to geometry of motion

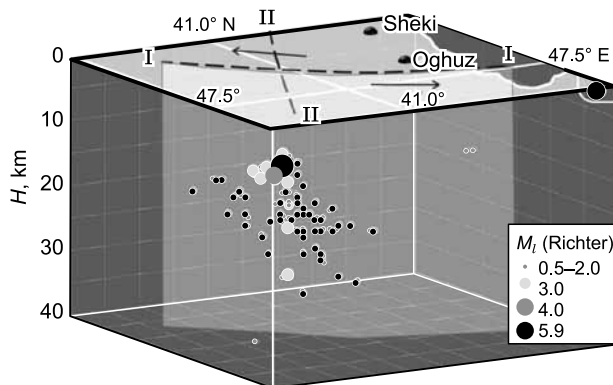


**Fig. 14.** 3D model of the aftershock field of the  $M_l = 5.9$  Oghuz earthquake of 4 September 2015. Faults: I, Arpa–Samur; II, North Ajinohur.

(normal, reverse, and strike slip) and compared in terms of source parameters. Histograms in Figs. 16 and 17 present parameters of motion for fifteen events. The  $PL$  difference does not exceed  $20^\circ$  in nearly 80% and 40% of cases for  $T$  and  $P$  axes, respectively. The axes of principal extension mainly have SW or NE orientations and those of compression are oriented in the NE–SW (67%) and NW–SE (33%) directions. The slip planes of different geometries are quite steep ( $>45^\circ$ ), which agrees with the  $50$  to  $90^\circ$  dips of most faults in the region. The plunge of NP1 ranges from  $-15^\circ$  to  $-43^\circ$  in 27% of events and from  $-57^\circ$  to  $-180^\circ$  in 40% of cases; the respective range for NP2 is  $-62^\circ$  to  $-171^\circ$  in 60% of sources. The variations of principal stress directions and fault plane angles, along with large standard deviations of the values, indicate considerable lithospheric heterogeneity.

The results were used to map compression and extension directions for the discussed large earthquakes. The principal compression changes direction from NW–SE in the Zaqatala area and N–S in the Sheki area clockwise to NE–SW in the Caspian Sea. The principal extension mainly follows the NE–SW and N–S directions in agreement with the major regional extension structure of the Kura basin subsiding beneath the Greater Caucasus along the Main Caucasian thrust fault (Fig. 18).

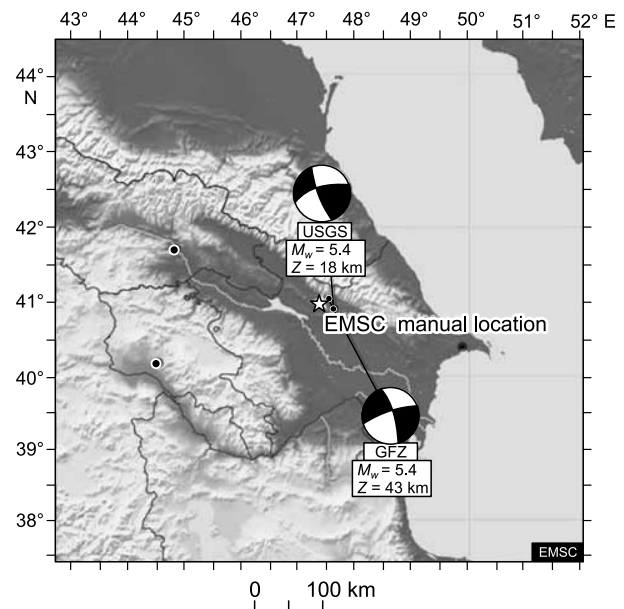


**Fig. 15.** Mechanisms of the Oghuz earthquakes according to USGS and GFZ agencies.

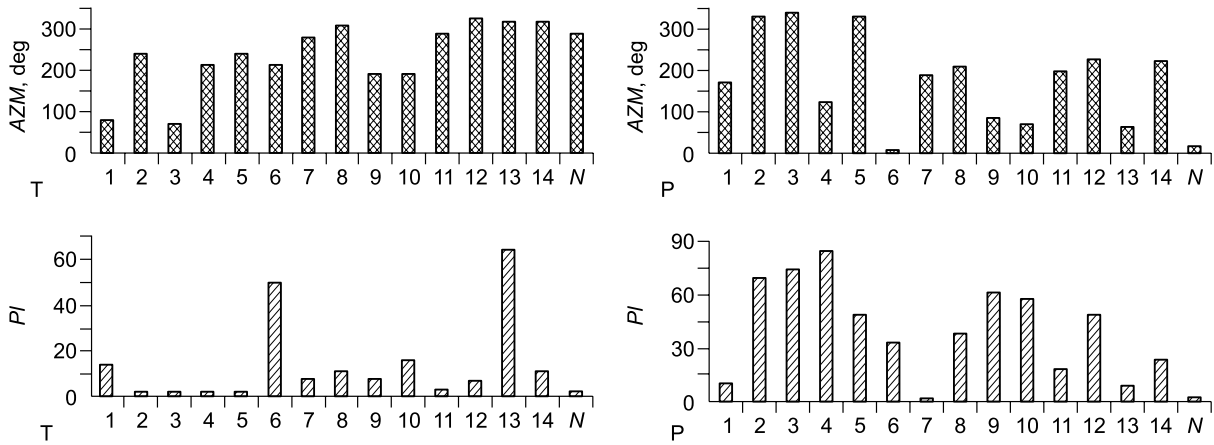


Fig. 16. Histograms of stress orientation parameters.

The earthquake sources are all related in a certain way. The similarity of the *DP*, *SLIP* and *STK* angles of reverse and thrust faults may indicate that motion occurred on the planes of the same faults. The Zaqatala earthquake may have triggered a number of large events in the Balakan, Sheki, Oghuz, Qabala, and Ismayilly areas which are subject to similar seismotectonic conditions. All these zones involve structural elements of the Tufan and Vandam uplifts, the Zaqatala–Hovdagh basin, and the superposed Alazani–Agrichay foredeep. These structures striking generally along the Caucasian Range are separated from one another by deep W–E faults (Shikhalibeili, 1996).

The origin depths of almost all large ( $M \geq 5.0$ ) earthquakes in Azerbaijan, including the Zaqatala and Balakan

events, correspond to the basement top (Mammadli, 2012). The Ismayilly earthquake is an exception: it originated as deep as 41 km while the depth to basement is 10–12 km (Fig. 19). Note that other small and medium events in the Ismayilly area had hypocenters at ~40 km. The large origin depths of earthquakes in the area may result from complex fault tectonics and requires further investigation (Yetirmishli et al., 2013). The earthquake sources of the study region are adjacent to the Iran seismic zone (Fig. 19) where earthquakes originate at depths from 5 to 20 km. Two  $M = 6.4$  events of 11 August 2012 in this zone, with origin depths of 10 km, were followed by numerous aftershocks that still continue nowadays.

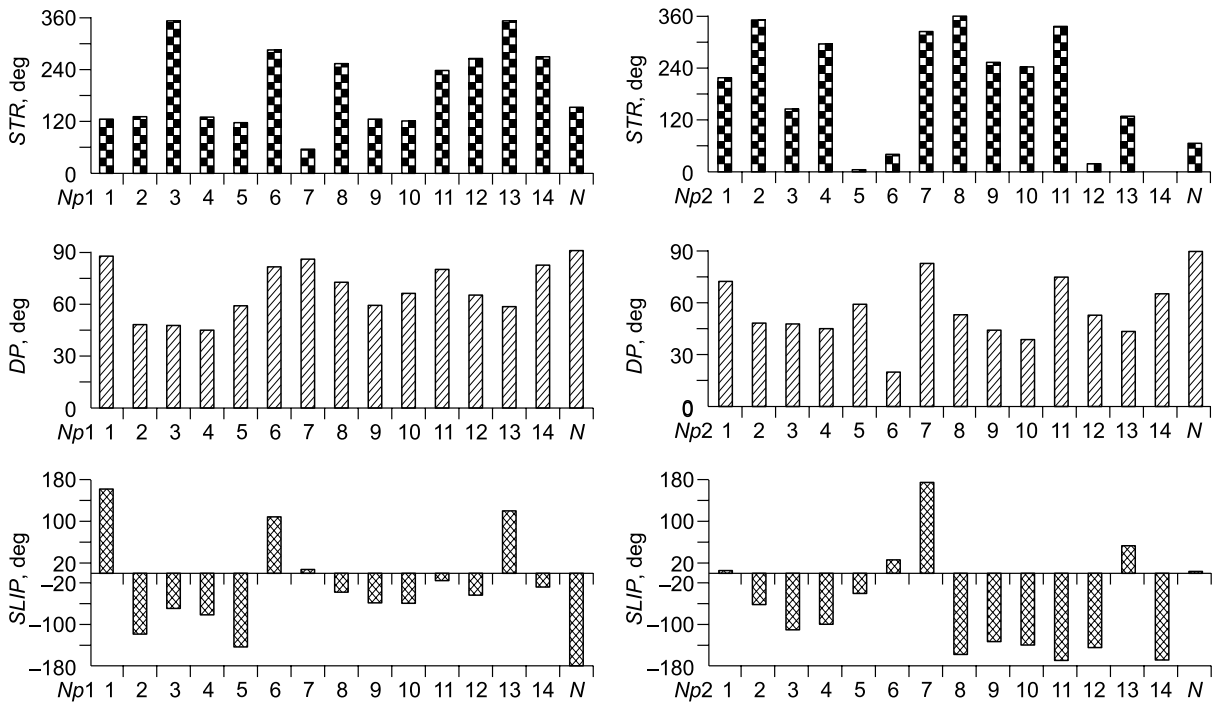


Fig. 17. Histograms of nodal plane parameters.

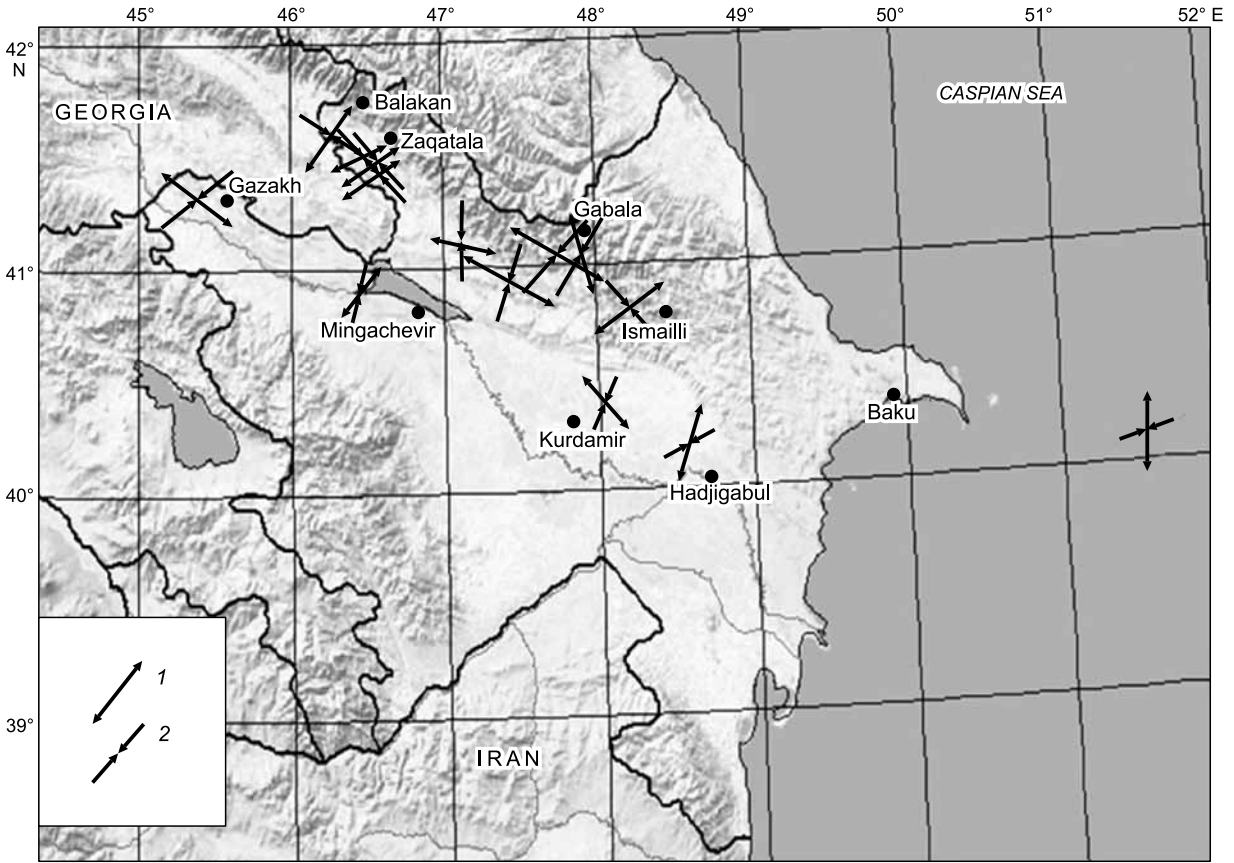


Fig. 18. Distribution of compression and extension and earthquake mechanisms, 2012–2015. 1, extension; 2, compression.

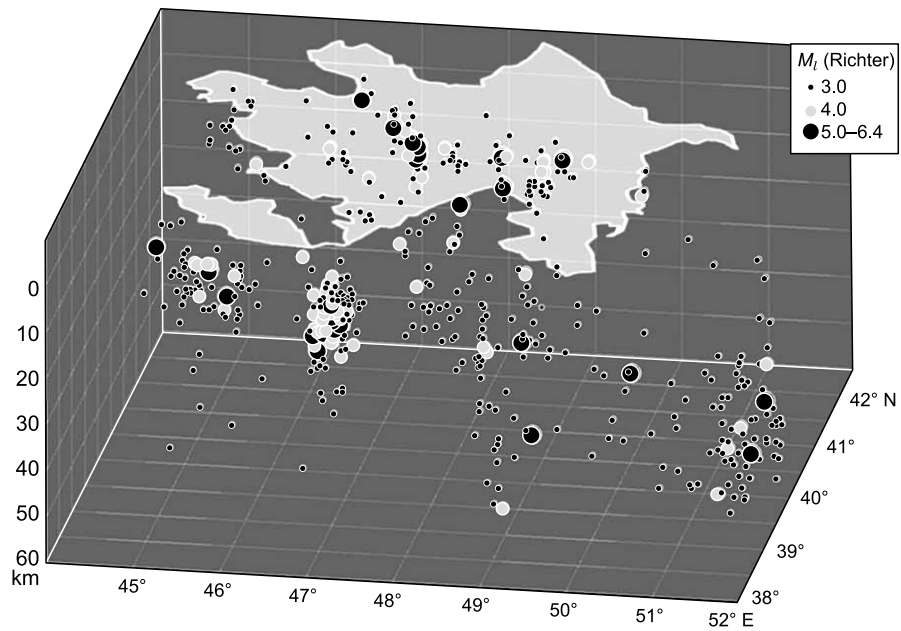


Fig. 19. 3D model of  $M_l \geq 3.0$  earthquake hypocenters in Azerbaijan, 2012–2015.

## CONCLUSIONS

The full waveform inversion of broadband digital data with the Time-Domain Moment Tensor INVerseCode (TDMT INVC) algorithm led to seismic-moment tensor solutions for earthquakes that occurred in Azerbaijan from 2012 through 2015. The results reveal typical features of seismotectonic deformation in the Zaqatala, Sheki, Qabala, Oghuz, Hacıqabul, İsmayilly, and Caspian Sea active seismic zones of the region.

The seismicity of the Greater Caucasus and the central Caspian Sea in 2012–2015 was associated with the activity of several large high-angle faults running along and across the main Caucasus Range. They are, namely, the faults of Gazakh–Signagi (SE, dipping at 72°), Ganjachay–Alazani (NW, 58°), Arpa–Samur (NE, 85°–90°, depths 16–25 km), İsmayilly–Qabala (SE, 44°, depth 46 km, and 53°, depth 11 km), as well as Goychay (NE, 81°), Mingachevir–Saatli (NE, 53°), and Absheron–Balkan (SW, 66°). The Zaqatala earthquakes associated with the activity of the cross-Caucasian Gazakh–Signagi and Ganjachay–Alazani right-lateral strike-slip faults may have been triggers for subsequent large shocks in the area. Statistical analysis of earthquake focal mechanisms shows predominance of horizontal extension and related activity of faults all over Azerbaijan.

The principal extension stress axes are oriented mainly in the SW and NW directions while the directions of compression are NE–SW in 67% of events and NW–SE in 33% of cases. The fault planes are rather steep ( $PL > 45^\circ$ ). This result agrees with the known 50°–90° dip angles of fault planes in the region, such as in the Gazakh–Signagi, Arpa–Samur, and Ganjachay–Alazani cross-Caucasian faults which dip within 58°–87° to depths from 9 to 20 km.

The summary of origin depths of earthquakes that shook Azerbaijan for the 2012–2015 period shows that most of the  $M \geq 5.0$  events originated on the basement surface (the Zaqatala and Balakan earthquakes agree with this trend), except for the İsmayilly earthquake that originated as deep as 41 km, while the depth to the basement is 10–12 km. The inferred directions of compression are NW–SE in the Zaqatala area and N–S in the Sheki area changing gradually clockwise to NE–SW in the Caspian Sea. The extension axis is mainly directed to NE–SW and N–S being associated with subsidence of the Kura basin beneath the Greater Caucasus along the Main Caucasian thrust fault.

## REFERENCES

- Akhmedbeili, F.S., İsaeva, M.I., Kadyrov, F.A., Korobanov, V.V., 2010. Neotectonic History of the Caucasus Segment of the Alpine–Himalayan Orogenic Belt [in Russian]. Nafta Press, Baku.
- Aslanov, B.S., 2009. Tectonics of Main Structural Elements in Azerbaijan and Their Expression in the Gravity Field [in Russian]. Author's Abstract. Doctor Thesis, Tashkent.
- Dreger, D.S., 2002. Time-Domain Moment Tensor INVerseCode (TDMT\_INVC). University of California, Berkeley Seismological Laboratory.
- Kengerli, T.N., 2007. Geology and tectonics of the southeastern Caucasus and petroleum potential problems. *Elmi Əsərlər*, No. 9, 3–12.
- Kerimov, K.M., Shikhalibeli, E.Sh., 1992. 1:1,000,000 Map of Deep Structure in the Black Sea–South Caspian Area [in Russian]. Baku.
- Kushnir, A.F., Rozhkov, M.V., Savin, E.A., Chebotareva, I.Ya., 2010. Scalable real-time seismic monitoring system based on SNDA problem-oriented algorithmic environment for man-caused and natural hazard assessment: practical results and perspectives. *Vestnik KRAUNTs. Nauki o Zemle*, No. 2 (Issue 16), 133–145.
- Mamedov, A.V., Gasanov, İ.S., İsmail-zade, A.D., 2005. Kura intermountain depression, in: Khain, V.E., Alizade, Ak.A. (Eds.), *Geology of Azerbaijan, Vol. IV: Tectonics* [in Russian]. Nafta-Press, Baku, pp. 214–234.
- Mammadli, T.Ya., 2012. Seismogenic zones in Azerbaijan and their deep structure, in: *Earthquake Prediction in Azerbaijan* [in Russian], pp. 287–295.
- Melnikova, V.I., Radziminovich, N.A., 1999. Earthquake Mechanisms in the Baikal Region [in Russian]. [http://seis-bykl.ru/modules.php?name=Seismo\\_mo](http://seis-bykl.ru/modules.php?name=Seismo_mo).
- Metaksas, Kh.P., Rzaev, A.G., İsaeva, M.I., 2011. Seismic risk parameters of the Shamakhi–İsmayilly source area, in: *Azərbaycan Ərazisində Seysmoproqnoz Müşahidələrin Kataloqu*, pp. 350–359.
- Rzaev, A.G., Metaksas, Kh.P., 2011. The Zaqatala earthquake of 7 May 2012: puzzles of the geodynamic regime and seismic-magnetic effect, in: *Azərbaycan Ərazisində Seysmoproqnoz Müşahidələrin Kataloqu*, pp. 350–359.
- Rzaev, A.G., Yetirmishli, K.J., Kazimova, S.E., 2013. Geodynamic regime expressed in geomagnetic field variations: a case study of the southern slope of the Greater Caucasus. *Izvestiya, Nauki o Zemle*, No. 4, 3–15.
- Shikhalibeli, E.Sh., 1996. Some Problems of Geology and Tectonics in Azerbaijan [in Russian]. Elm, Baku.
- Sycheva, N.A., 2004. Features of Earthquake Mechanisms and Seismotectonic Deformation in the Northern Tien Shan, from Data of the KNET Seismic Network. Author's Abstract, Candidate Thesis [in Russian]. IPE RAS, Moscow.
- Yetirmishli, G.D., Kazimova, S.E., 2012. The crustal velocity model of Azerbaijan from Digital Seismic Data. *Geologiya i Geofizika Yuga Rossii*, No. 1, 59–73.
- Yetirmishli, G.C., Mammadli, T.Y., Kazimova, S.E., 2013. Features of seismicity of Azerbaijan part of the greater Caucasus, *J. Geogr. Geophys. Soc., Issue (A), Phys. Solid Earth* 16a, 55–60.

*Editorial responsibility: V.S. Seleznev*